ones that are similar to those being developed for the fabrication of (bio)sensors. Note that the wavelength is determined by the different rate constants, which can be varied, e.g., by choosing different faradaic reactions or adsorbates or by changing the temperature. In general, the faster the faradaic reaction and the dynamics of the adsorbate system, the smaller are the patterns. Therefore, at least to a certain extent, the size of the patterns can be controlled by carefully choosing the reaction conditions. Also, electrochemical membrane systems exhibit a first-order phase transition (*20*). In many investigations, the degree of inhibition of an electron-transfer reaction serves as a measure of the intactness of the membrane. To be aware of the spatial instability discussed above is thus essential for understanding the dynamics of these lipid layers coupled to faradaic reactions. This, in turn, is the basis for using electrochemical membrane systems as models of biological membranes, e.g., in investigations of the role of the potential on the membrane-protein interactions (*21*, *22*).

Turing's conditions are fulfilled in chemical reaction-diffusion systems only in exceptional cases, whereas the new class of Turing-type structures in electrochemical systems is predicted to arise quite generally. This finding opens prospects toward tailoring of patterned electrodes. It remains further to be examined whether the same mechanism is responsible for some structure formation phenomena in a biological environment where potential gradients exist.

References and Notes

1. A. M. Turing, *Philos. Trans. R. Soc. London* **237**, 37 (1952).
2. R. Kapral, K. Showalter, Eds., *Chemical Waves and Patterns* (Kluwer, Dordrecht, Netherlands, 1995).
3. J. D. Murray, *Mathematical Biology* (Springer, Berlin, 1990).
4. G. Nicolis, *Introduction to Nonlinear Science* (Cambridge Univ. Press, Cambridge, 1995).
5. J. Ross, A. P. Arkin, S. C. Müller, *J. Chem. Phys.* **99**, 10417 (1995).
6. V. Castets, E. Dulos, J. Boissonade, P. deKepper, *Phys. Rev. Lett.* **64**, 2953 (1990).
7. I. R. Epstein, I. Lengyel, S. Kádár, M. Kagan, M. Yokoyama, *Physics A* **188**, 26 (1992).
8. Q. Ouyang, H. L. Swinney, *Nature* **352**, 610 (1991).
9. I. Lengyel, I. R. Epstein, *Proc. Natl. Acad. Sci. U.S.A.* **89**, 3977 (1992).
10. N. Mazouz, K. Krischer, *J. Phys. Chem. B* **104**, 6081 (2000).
11. The term reflects the fact that when connecting the ends of the two stable states of the bistable region of the I-ϕ_{DL} curve, the two stable branches together with the connecting line form an S shape. A second type of bistable I-ϕ_{DL} curve gives rise to a Z shape (compare with Fig. 2C).
12. G. Flätgen *et al.*, *Science* **269**, 668 (1995).
13. H. Striegler, thesis, Universität Ulm, Germany (1998).
14. N. Mazouz, G. Flätgen, K. Krischer, *Phys. Rev. E* **55**, 2260 (1997).
15. M. Hildebrand, A. Mikhailov, G. Ertl, *Phys. Rev. E* **68**, 5483 (1998).
16. B. A. Hubermann, *J. Chem. Phys.* **65**, 2013 (1976).
17. A. Mikhailov, G. Ertl, *Chem. Phys. Lett.* **238**, 104 (1995).
18. J. Verdasca, P. Borckmans, G. Dewel, *Phys. Rev. E* **52**, R4616 (1995).
19. Reviewed in C. Buess-Herman, *Prog. Surf. Sci.* **46**, 335 (1994).
20. D. Bizzotto, A. Nelson, *Langmuir* **14**, 6269 (1998).
21. D. Bizzotto, E. Wang, Y. Yang, *J. Electroanal. Chem.* **480**, 233 (2000).
22. M. Rueda *et al.*, *Langmuir* **15**, 3672 (1999).

23. We are grateful to D. M. Kolb and H. Striegler for discussions on camphor adsorption on Au electrodes and to A. Martin (Fritz-Haber-Institut) for preparing the Au films. Supported by the Deutsche Forschungsgemeinschaft, in the framework of the Sfb 555/B4.

28 November 2000; accepted 13 February 2001
Published online 22 February 2001;
10.1126/science.1057830
Include this information when citing this paper.

Biogenic Carbon Cycling in the Upper Ocean: Effects of Microbial Respiration

Richard B. Rivkin[1]* and Louis Legendre[2]

Food-web processes are important controls of oceanic biogenic carbon flux and ocean-atmosphere carbon dioxide exchange. Two key controlling parameters are the growth efficiencies of the principal trophic components and the rate of carbon remineralization. We report that bacterial growth efficiency is an inverse function of temperature. This relationship permits bacterial respiration in the euphotic zone to be computed from temperature and bacterial production. Using the temperature-growth efficiency relationship, we show that bacterial respiration generally accounts for most community respiration. This implies that a larger fraction of assimilated carbon is respired at low than at high latitudes, so a greater proportion of production can be exported in polar than in tropical regions. Because bacterial production is also a function of temperature, it should be possible to compute euphotic zone heterotrophic respiration at large scales using remotely sensed information.

The net flux of CO_2 between the atmosphere and ocean is controlled, in large part, by the balance among three key food-web processes: carbon uptake by phytoplankton photosynthesis (PP, net primary production), its remineralization back to CO_2 (CR, community heterotrophic respiration in the euphotic zone), and the export (E) of dissolved and particulate biogenic carbon (BC) toward the ocean depths. Although phytoplankton production and, to a lesser extent, export are reasonably well defined for large ocean areas (*1*), the regional estimates of respiration that are necessary to constrain both export ($E = PP - CR$) and the net ocean-atmosphere exchange of CO_2 are often lacking (*2*). Community respiration, of which bacterial respiration (BR) can represent a large proportion [~50 to >90% (*3*–*5*)], can exceed primary production in some ocean regions (*6*–*9*). Hence, bacterial respiration may constrain the estimates of both carbon remineralization and biogenic carbon export in the upper ocean (*7*). Because of methodological difficulties, bacterial respiration is usually not measured directly and is instead computed from bacterial production (BP) and an assumed value of bacterial growth efficiency (BGE)

$$BGE = BP/B_{DOC} \quad (1)$$

Bacterial growth efficiency is the ratio of bacterial production to substrate assimilated (B_{DOC}), and since the assimilated dissolved organic carbon (DOC) is used for both the synthesis of bacterial biomass and is respired (i.e., $B_{DOC} = BP + BR$), bacterial growth efficiency can also be computed as

$$BGE = BP/(BP + BR) \quad (2)$$

Hence

$$BR = (BP/BGE) - BP \quad (3)$$

The estimation of bacterial respiration from Eq. 3 has been limited until now because of large variations reported for bacterial growth efficiencies [0.01 to ~0.7 (*5, 9, 10*)]. These variations introduce large uncertainties into the computation of bacterial respiration. For example, for the twofold range of growth efficiencies (e.g., 0.25 to 0.5) assumed in many studies (*6, 9, 11*), respiration would change by threefold. It follows that the use of a realistic bacterial growth efficiency is crucial to constraining rates and patterns of carbon remineralization, food-web fluxes of biogenic carbon, and ocean-atmosphere flux of CO_2 (*2, 6, 8*).

We carried out a comprehensive review of the literature on bacterial growth efficiency (*12, 13*) and found a significant ($P < 0.001$) inverse

[1]Ocean Sciences Centre, Memorial University of Newfoundland, St. John's, Newfoundland A1C 5S7, Canada. [2]Laboratoire d'Océanographie de Villefranche, Boîte Postale 28, 06234 Villefranche-sur-Mer Cedex, France.

*To whom correspondence should be addressed. E-mail: rrivkin@mun.ca

relation between temperature (T) and growth efficiency (Fig. 1). Temperature alone explained 54% of the variation in bacterial growth efficiency. A portion of the unexplained variance could be due to regional and seasonal differences in the quality and quantity of mineral and organic substrates required for bacterial growth (*10, 14, 15*). Because culture studies with bacteria growing on defined substrates also show significant ($P < 0.01$) inverse relationships between growth efficiency and temperature (*16*) it is unlikely that the observed significant relation between growth efficiency and temperature (Fig. 1) is a data-collection artifact created by combining data from different sites or seasons. Moreover, temperature dependence of growth efficiency is not unique for bacteria. Phagotrophic protists, a major group of heterotrophic microplankton in the sea (*17*), show a similar temperature dependence of growth efficiency. The temperature-growth efficiency relationship for flagellates and ciliates from a variety of high- and low-latitude marine environments was significant ($P < 0.01$) and inverse (*18*). Prey type and food concentration influences the growth efficiency of protistan grazers (*19*), and during experiments where temperature was the sole treatment variable, it explained >70% of variation in growth efficiency (*20–24*).

The slopes of the regression of growth efficiency on temperature were not significantly different ($\alpha = 0.05$) for phagotrophic protists and bacteria (Fig. 1) (*18*), suggesting a similar temperature dependence for these two groups of ecologically important microheterotrophs. The temperature dependence suggests that there is a latitudinal gradient in the partitioning of the assimilated (bacteria) or ingested (phagotrophic protists) carbon between biomass production and respiration—i.e., a larger fraction of this carbon is respired at lower latitudes. Thus, for the same level of bacterial or phytoplankton production, the food web and vertical export of biogenic carbon would be greater in polar than in tropical regions. Moreover, the higher growth efficiency at lower ambient temperatures would lead to a higher activity of bacterial-based food webs in polar waters than would be predicted from temperature-dependent models developed from studies in temperate oceans. Incorporation of these new relationships into biogeochemical models could profoundly influence our estimates of global carbon cycling and remineralization by marine food webs.

Modeling studies that predict increasing temperatures in the low atmosphere and surface-ocean in response to increased concentrations of atmospheric CO_2 also suggest that the oceanic biogeochemical cycles may partially mitigate the accumulation of atmospheric CO_2 on centennial time scales (*25, 26*). Small changes in the oceanic carbon cycle can produce large changes in the rate of buildup or removal of atmospheric CO_2, thereby impacting the future climate. Because there is an inverse relationship between temperature and both growth efficiency (~2.5% decrease per 1°C increase; Fig. 1) and solubility of CO_2 in seawater [~3% decrease per 1°C increase (*27*)], an increase in sea-surface temperature may lead to an increase in the proportion of the assimilated carbon that is remineralized to CO_2 (due to changes in bacterial growth efficiency) and to a reduction in the solubility of CO_2. This form of positive feedback between increased temperature and changes in the patterns of CO_2 cycling in the upper ocean has not been generally considered in models of biogenic carbon cycling and ocean-atmosphere interactions (*28*).

Region- to basin-scale estimates of community respiration and primary production can constrain both net community production (NCP) and export (i.e., NCP = E = PP – CR). However, because measurements of respiration are scarce relative to primary production, the application of this approach will require the development of models to estimate community respiration over large spatial and temporal scales. Temperature has a pronounced effect on the rates of both individual and community metabolism, so that temperature and respiration are correlated (*29, 30*). Empirical models of community and bacterial respiration have been developed with phytoplankton or bacterial production or biomass as predictors (*9, 10, 31, 32*). However, to our knowledge, the predictive abilities of the empirical models of respiration have not been assessed with independent data sets. If bacterial respiration, computed from Eq. 3 and bacterial production

$$BR = [BP/(0.374 - 0.0104T)] - BP \quad (4)$$

does indeed represent a large or constant portion of community respiration, it may be possible to estimate carbon remineralization rates for large regions of the World Ocean from bacterial production [which is reasonably well characterized for coastal and oceanic environments (*11, 33*)] and temperature. Using a data set (*34*) that was completely independent from that of Fig. 1, we found that the functional relationship between computed bacterial respiration and field-measured community respiration (Fig. 2) was significant over a wide range of observed temperatures (–1.4 to 29°C), rates of bacterial production (0.2 to 415 mg C m^{-3} d^{-1}), and community respiration (1.8 to 2300 mg C m^{-3} d^{-1}). The results of this analysis (Fig. 2; slope = 1.10 and $r^2 = 0.88$) suggests that, for a wide range of conditions, bacterial respiration estimated from bacterial production and temperature (Eq. 4) is a valid proxy for respiration (*35*). We show that bacterial growth efficiency can be estimated from temperature (Fig. 1). Bacterial production, the other variable needed to compute respiration, is correlated with both temperature ($r^2 = 0.55$) and chlorophyll a ($r^2 = 0.36$) (*36*). It should be possible to concurrently estimate community respiration (Fig. 2) (*34*) and primary production (*37*) and thus compute carbon export for large areas of the World Ocean from remotely sensed temperature and chlorophyll a values (*37*).

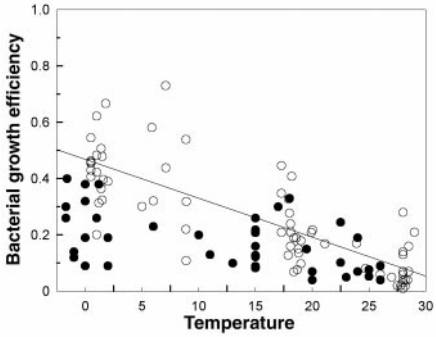

Fig. 1. Scatter plot of bacterial growth efficiency as a function of temperature for bacterioplankton from polar, temperate, and tropical oceans. Bacterial growth efficiency was determined from concurrent measurements of bacterial production and DOC uptake (open symbols) or of bacterial production and size-fractionated O_2 uptake (filled symbols). The ordinary least squares regression (regression line shown) between temperature (T) and bacterial growth efficiency (BGE) is: BGE = 0.374[±0.04] – 0.0104[±0.002]T, ($r^2 = 0.54$, $n = 107$, $F = 84.27$, $P < 0.001$). Values in brackets are the 95% confidence intervals of the regression parameters.

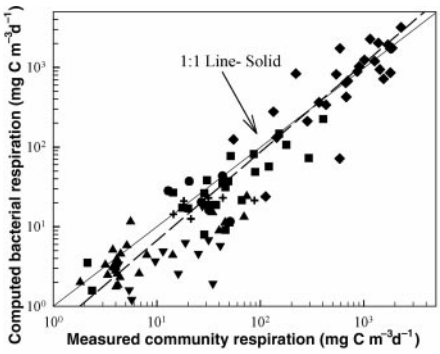

Fig. 2. Scatter plot of field-measured community respiration versus computed bacterial respiration for the Antarctic (+), Arctic (▼), Arabian Sea (●), Gulf of Mexico (■), North Atlantic (▲), and South Atlantic Bight (◆). The solid 1:1 line is shown for visual reference. Using the database described in (*34*), bacterial respiration was computed from the reported bacterial production and ambient temperature using Eq. 4. The data were log-transformed to normalize variances. The structural (reduced major axis) regression (dashed line) between field-measured community respiration (CR) and computed bacterial respiration (C-BR) is: Log C-BR = –0.36[±0.13] + 1.10[±0.08] Log CR, ($r^2 = 0.88$, $n = 100$, $F = 738.8$, $P < 0.0001$). Values in brackets are the 95% confidence intervals of the regression parameters. The slope (1.14), r^2 (0.81), and significance ($F = 404.8$, $P < 0.0001$) of the structural relationship between measured community respiration versus computed bacterial respiration for the raw (i.e., nontransformed) data were similar to those for the log-transformed data.

References and Notes

1. P. G. Falkowski, R. T. Barber, V. Smetacek, *Science* **281**, 200 (1998).
2. P. J. le B. Williams, in *Microbial Ecology of the Oceans*, D. L. Kirchman, Ed. (Wiley, New York, 2000), pp. 153–200.
3. P. J. le B. Williams, in *Heterotrophic Activity in the Sea*, J. E. Hobbie, P. J. le B. Williams, Eds. (Plenum, New York, 1983), pp. 375–389.
4. E. B. Sherr, B. F. Sherr, *Aquat. Microb. Ecol.* **11**, 91 (1996).
5. R. A. Jahnke, D. B. Craven, *Limnol. Oceanogr.* **40**, 436 (1995).
6. P. A. del Gorgio, J. J. Cole, in *Microbial Ecology of the Oceans*, D. L. Kirchman, Ed. (Wiley, New York, 2000), pp. 289–325.
7. P. J. le B. Williams, *Nature* **394**, 55 (1998).
8. C. Duarte, S. Agusti, *Science* **281**, 234 (1998).
9. P. A. del Gorgio, J. J. Cole, A. Cimbleris, *Nature* **385**, 148 (1997).
10. P. A. del Gorgio, J. J. Cole, *Annu. Rev. Ecol. Syst.* **29**, 503 (1998).
11. H. W. Ducklow, C. A. Carlson, *Adv. Microb. Ecol.* **12**, 113 (1992).
12. The relationship between temperature and growth efficiency for marine bacterioplankton from a wide range of oceanic sites was assessed using published data (*38*). We restricted the data set to bacterial growth efficiency determined from concurrent measurements of bacterial production and DOC uptake or bacterial production and size-fractionated ($<$1.0 or 0.8 μm) O_2 uptake (assuming that $<$1.0 μm community respiration was equivalent to bacterial respiration). Bacterial growth efficiency estimated from the metabolism of single or simple combinations of radiolabeled substrates (e.g., ^{14}C-labeled glucose, amino acids, etc.), determined during nutrient-enrichment experiments or computed from bacterial production and non–size fractionated community respiration were not included in our analysis (*6, 10*). Even with this constraint, we obtained 107 paired observations of temperature and bacterial growth efficiency from polar, temperate, and subtropical oceans. Approximately 20%, 40%, and 75% of observations were from $\leq$1°C, $<$10°C and $<$20°C, respectively. Mean, median, and ranges of temperature and bacterial growth efficiency were 14°C, 17°C, and –1.7 to 29°C, respectively, and 0.23, 0.19, and 0.01 to 0.73, respectively. Previous analyses of the temperature dependence of bacterial growth efficiency (*10*) were biased toward higher temperatures (mean = 19°C), with few data below 10°C.
13. Although some individual studies report that bacterial growth efficiency increases with a seasonal increase in temperature, most studies show the opposite trend (Fig. 1) [Web table 1 (*38*)]. All studies containing concurrent measurements of temperature and bacterial growth efficiency (regardless of the temperature–bacterial growth efficiency trend) were included in the analysis reported in (*12*) and shown in Fig. 1.
14. W. J. Payne, W. J. Weibe, *Annu. Rev. Microbiol.* **32**, 155 (1974).
15. T. R. Anderson, *J. Plankton Res.* **14**, 1645 (1992).
16. Temperature alone explained 77 to 94% of the variance in growth efficiency for two strains of *Vibrio* (*39, 40*).
17. P. C. Reid, C. M. Turley, P. H. Burkhill, *Protozoa and Their Role in Marine Processes* (Springer Verlag, New York, 1988).
18. The temperature–growth efficiency (GE) relationship for marine phagotrophic flagellates and ciliates was examined using 63 paired observations of temperature and growth efficiency from eight published papers. Growth efficiency was generally determined from concurrent measurements of the production of protistan biomass and the ingestion of algal or bacterial prey carbon. Approximately 7%, 16%, and 45% of the observations were from $<$4°C, $<$10°C, and $<$20°C, respectively. Mean, median, and ranges for temperature and growth efficiency were 15.2°C, 14°C, and $-$1.5 to 26°C, respectively and 0.40, 0.41, and 0.10 to 0.71, respectively. The inverse linear relationship between temperature and growth efficiency is described by the linear least squares regression: GE = 0.66[$\pm$0.071] – 0.014[$\pm$0.004]T, (r^2 = 0.41, n = 63, $P < 0.01$). Values in brackets are the 95% confidence intervals of the regression parameters.
19. D. Straile, *Limnol. Oceanogr.* **42**, 1375 (1997).
20. The coefficients of determination of the temperature–growth efficiency relationship for flagellate *Paraphysomonas imperforata* ingesting bacterial and algal prey was r^2 = 0.71 to 0.89 (*22, 23*). Similar high coefficients of determination were reported for the herbivorous ciliates *Tintinnopsis* [r^2 = 0.87 to 0.94 (*24*)] and *Lomanniella* [r^2 = 0.89 to 0.96 (*25*)].
21. D. A. Caron, J. C. Goldman, M. R. Dennett, *Appl. Environ. Microbiol.* **52**, 1340 (1986).
22. J. W. Choi, F. Peters, *Appl. Environ. Microbiol.* **58**, 593 (1992).
23. P. G. Verity, *Limnol. Oceanogr.* **30**, 1268 (1985).
24. F. Rassoulzadegan, *Ann. Inst. Oceanogr. Paris* **58**, 177 (1992).
25. J. L. Sarmiento, C. LeQuéré, *Science* **274**, 1346 (1996).
26. J. L. Sarmiento, T. M. C. Hughes, R. L. Stouffer, S. Manabe, *Nature* **393**, 245 (1998).
27. R. F. Weiss, *Mar. Chem.* **2**, 203 (1974).
28. J. Woods, W. Barkmann, *J. Plankton Res.* **15**, 1053 (1993).
29. P. Sampou, W. M. Kemp, *Mar. Ecol. Prog. Ser.* **110**, 240 (1994).
30. D. Lefèvre *et al.*, *J. Exp. Mar. Biol. Ecol.* **184**, 201 (1994).
31. L. Jensen, K. Sand-Jensen, S. Marcher, M. Hansen, *Mar. Ecol. Prog. Ser.* **61**, 75 (1990).
32. J. W. Fourqurean, K. L. Webb, T. Hollibaugh, S. V. Smith, *Estuarine Coastal Shelf Sci.* **44**, 493 (1997).
33. H. W. Ducklow, *FEMS Microbiol. Ecol.* **30**, 1 (1999).
34. We constructed a database from the published literature which contained concurrent sets of values of euphotic zone temperature and rates of bacterial production and community respiration (determined from O_2 uptake by the whole planktonic community) from polar, temperate, and tropical oceanic and coastal sites [Web table 2 (*38*)]. For data reported in areal units, euphotic zone average volumetric values were computed by dividing by the integration depth. For data reported in volumetric units, vertical profiles were integrated over the depth of the euphotic zone, and then divided by the integration depth. This data set (n = 100 profiles) was independent of that used to assess the temperature–bacterial growth efficiency relationship (Fig. 1). From temperature and bacterial production, we computed bacterial respiration using Eq. 4, and compared these estimates with the concurrent measurements of community respiration.
35. Although bacterial respiration computed from Eq. 4 was occasionally lower than measured community respiration, the rates were not significantly different (paired t-test; P = 0.79) and computed bacterial respiration was always with the 95% confidence interval of the regression estimate.
36. P. A. White, J. Kalff, J. B. Rasmussen, J. M. Grasol, *Microb. Ecol.* **21**, 99 (1991).
37. S. Sathyendranath *et al.*, *Nature* **353**, 129 (1991).
38. Supplementary Web data is available at www.sciencemag.org/cgi/content/full/291/5512/2398/DC1
39. R. R. Christian, W. J. Weibe, *Can. J. Microbiol.* **20**, 1341 (1974).
40. R. A. Herbert, C. R. Bell, *Arch. Microbiol.* **113**, 215 (1977).

41. We thank M. R. Anderson, D. Deibel, L. Johnson, B. Klein, and C. Robinson for helpful comments and discussions, and P. Matthews and J. Michaud for assistance in assembling the databases. Supported by Research Grants to R.B.R. and L.L. from the Natural Sciences and Engineering Council of Canada.

6 June 2000; accepted 21 February 2001

Variation of Crystal Dissolution Rate Based on a Dissolution Stepwave Model

Antonio C. Lasaga[1] and Andreas Luttge[2]*

A formulation based on defect-generated dissolution stepwaves of the variation of dissolution rate with the degree of undersaturation is validated by near-atomic-scale observations of surfaces, Monte Carlo simulations, and experimental bulk dissolution rates. The dissolution stepwaves emanating from etch pits provide a train of steps similar to those of a spiral but with different behavior. Their role in accounting for the bulk dissolution rate of crystals provides a conceptual framework for mineral dissolution far from equilibrium. Furthermore, the law extends research to conditions closer to equilibrium and predicts a nonlinear decrease in the rate of dissolution as equilibrium is approached, which has implications for understanding artificial and natural processes involving solid-fluid reactions.

The dissolution of minerals is central to a wide range of engineering, pollution, corrosion, and Earth science phenomena. Whether it be the weathering of rocks to form soils and control CO_2 in the atmosphere, the possible reaction of radioactive containment materials, the breakdown of cement in buildings and dams, the leaching of aluminum or heavy metals in drinking water, or the flow of fluids deep in Earth's crust, no quantitative treatment is possible without an understanding of the kinetics of fluids reacting with solid surfaces. The lack of a general dissolution model means that the overall crystal dissolution rate and its variation with environmental conditions cannot be fully determined.

Historically, the science of crystal growth has advanced much more than that of crystal dissolution. The theory of surface-controlled crystal growth is dominated by an emphasis on the movement of steps and by two conceptual

[1]Department of Geology and Geophysics, Yale University, New Haven, CT 06520, USA. [2]Department of Earth Science, Rice University, Houston, TX 77005, USA.

*To whom correspondence should be addressed. E-mail: aluttge@rice.edu